# Performance enhancement of an InGaN light-emitting diode with an AlGaN/InGaN superlattice electron-blocking layer*

Xiong Jian-Yong(熊建勇)[a], Xu Yi-Qin(许毅钦)[b], Zhao Fang(赵 芳)[a], Song Jing-Jing(宋晶晶)[a], Ding Bin-Bin(丁彬彬)[a], Zheng Shu-Wen(郑树文)[a], Zhang Tao(张 涛)[a], and Fan Guang-Han(范广涵)[a]†

[a] *Laboratory of Nanophotonic Functional Materials and Devices, Institute of Optoelectronic Materials and Technology, South China Normal University, Guangzhou* 510631, *China*

[b] *Guangdong General Research Institute for Industrial Technology, Guangzhou* 510650, *China*

(Received 28 December 2012; revised manuscript received 9 April 2013)

The efficiency enhancement of an InGaN light-emitting diode (LED) with an AlGaN/InGaN superlattice (SL) electron-blocking layer (EBL) is studied numerically, which involves the light-current performance curve, internal quantum efficiency electrostatic field band wavefunction, energy band diagram carrier concentration, electron current density, and radiative recombination rate. The simulation results indicate that the LED with an AlGaN/InGaN SL EBL has better optical performance than the LED with a conventional rectangular AlGaN EBL or a normal AlGaN/GaN SL EBL because of the appropriately modified energy band diagram, which is favorable for the injection of holes and confinement of electrons. Additionally, the efficiency droop of the LED with an AlGaN/InGaN SL EBL is markedly improved by reducing the polarization field in the active region.

**Keywords:** light-emitting diodes, AlGaN/InGaN superlattice efficiency droop, numerical simulation

**PACS:** 85.60.Jb, 73.61.Ey, 78.60.Fi, 87.15.Aa **DOI:** 10.1088/1674-1056/22/10/108505

## 1. Introduction

The InGaN light-emitting diodes have been found to have tremendous potential as a pumping source for general illumination and full-color displays.[1,2] However, the efficiency droop needs to be further improved for LEDs to be competitive in terms of high-brightness and high-power applications. Several possible causes for the efficiency droop have been proposed, such as the quantum confined Stark effect (QCSE),[3] Auger recombination,[4] current crowding effect,[5] self-heating effect,[6] polarization effect,[7] and current injection efficiency.[8] Among the above causes, the main causes for the efficiency droop are presumably electron leakage and poor hole injection.[9,10] So far, many methods have been proposed to reduce the effect of electron current leakage[11–14] and to increase the efficiency of hole injection.[15–19] Even, some scientists have tried to use an AlGaN/GaN superlattice (SL) EBL to improve the performance of LEDs.[20] It has been proposed that an AlGaN/GaN SL EBL in an LED device structure could prevent the carrier loss over heterostructure barriers.[21,22] However, published research indicates that performance improvement by the normal AlGaN/GaN SL EBL in suppressing the spillover of electrons and increasing the hole injection efficiency is limited due to the severe band bending of the EBL caused by a strong electrostatic field generated by the lattice mismatch between the GaN and AlGaN interface.[23] Thus, the idea of an AlGaN/InGaN SL EBL is proposed for reducing polarization and achieving higher hole-injection efficiency. For the GaN template, the AlGaN layer has tensile strain and the InGaN layer has compressive strain. Hence, the use of an AlGaN/InGaN heterostructure is beneficial for strain relaxation and is quite feasible for epitaxy growth.[24]

## 2. Structure and parameters

The structure of the conventional LED (denoted as structure A) used in this paper as a reference was grown on a *c*-plane sapphire substrate, followed by a 50-nm-thick undoped GaN buffer layer, and a 4.5-μm-thick n-GaN layer (n-doping = $5 \times 10^{18}$ cm$^{-3}$). The active region consisted of five 2.2-nm-thick $In_{0.11}Ga_{0.9}N$ quantum wells (QWs), sandwiched by six 15-nm-thick GaN barriers. At the top of the active region were a 20-nm-thick p-$Al_{0.15}Ga_{0.85}N$ EBL (p-doping = $5 \times 10^{17}$ cm$^{-3}$) and a 0.2-μm-thick p-GaN cap layer (p-doping = $7 \times 10^{17}$ cm$^{-3}$). The device geometry was designed into a rectangular shape of 300 μm × 300 μm. Two other LED structures, which have an identical layer structure to the conventional structure except for the AlGaN EBL, were replaced by 10-period $Al_{0.15}Ga_{0.85}N$/GaN (1 nm/1 nm, p-doping = $5 \times 10^{17}$ cm$^{-3}$) SLs (denoted as structure B) and 10-period $Al_{0.15}Ga_{0.85}N/In_{0.03}Ga_{0.97}N$ (1 nm/1 nm, p-doping

*Project supported by the National Natural Science Foundation of China (Grant No. 61176043) and the Special Funds for Provincial Strategic and Emerging Industries Projects of Guangdong, China (Grant Nos. 2010A081002005, 2011A081301003, and 2012A080304016).

†Corresponding author. E-mail: gfan@scnu.edu.cn

© 2013 Chinese Physical Society and IOP Publishing Ltd 

$= 5 \times 10^{17}$ cm$^{-3}$) SLs (denoted as structure C), respectively.

The optical and electrical properties of the LEDs were investigated numerically with the advanced physical model of semiconductor devices (APSYS)[25] simulation software, which is developed by Crosslight Software Inc. APSYS software is capable of dealing with the physical properties of LEDs by solving the Poisson's equation, current continuity equations, carrier transport equation, quantum mechanical wave equation, and photon rate equation. Of course, it is necessary to take full account of the built-in charge density induced by the spontaneous and piezoelectric polarization within the interface of the InGaN light-emitting diodes because it plays an important part for nitride-based optical devices. The spontaneous polarization of the ternary nitride alloy can be calculated by the following formulas developed by Fiorentini *et al.*[26]

$$P_{\rm sp}({\rm In}x{\rm Ga}_{1-x}{\rm N}) = x \cdot P_{\rm sp}({\rm InN}) + (1-x) \cdot P_{\rm sp}({\rm GaN}) + B({\rm InGaN}) \cdot x \cdot (1-x), \quad (1)$$

$$P_{\rm sp}({\rm Al}x{\rm Ga}_{1-x}{\rm N}) = x \cdot P_{\rm sp}({\rm AlN}) + (1-x) \cdot P_{\rm sp}({\rm GaN}) + B({\rm AlGaN}) \cdot x \cdot (1-x), \quad (2)$$

where $P_{\rm sp}({\rm InN})$, $P_{\rm sp}({\rm GaN})$, and $P_{\rm sp}({\rm AlN})$ are spontaneous polarizations of InN, AlN, and GaN, with values of $-0.042$ C/m$^2$–$0.090$ C/m$^2$, and $-0.034$ C/m$^2$, respectively; $B$(InGaN) and $B$(AlGaN) are spontaneous polarization bowing parameters of InGaN and AlGaN, which are $-0.037$ C/m$^2$ and $-0.021$ C/m$^2$, respectively. On the other hand, the piezoelectric polarization of the ternary nitride alloys can be calculated by Vegard's interpolation which can be expressed as

$$P_{\rm pz}({\rm In}x{\rm Ga}_{1-x}{\rm N}) = P_{\rm pz}({\rm InN}) \cdot x + P_{\rm pz}({\rm GaN}) \cdot (1-x), \quad (3)$$

$$P_{\rm pz}({\rm Al}x{\rm Ga}_{1-x}{\rm N}) = P_{\rm pz}({\rm AlN}) \cdot x + P_{\rm pz}({\rm GaN}) \cdot (1-x), \quad (4)$$

where

$$P_{\rm pz}({\rm InN}) = -1.373 \cdot \varepsilon + 7.559 \cdot \varepsilon^2, \quad (5)$$

$$P_{\rm pz}({\rm GaN}) = -0.918 \cdot \varepsilon + 9.541 \cdot \varepsilon^2, \quad (6)$$

$$P_{\rm pz}({\rm AlN}) = -1.808 \cdot \varepsilon + 5.624 \cdot \varepsilon^2 \ \text{ for } \ \varepsilon < 0, \quad (7)$$

$$P_{\rm pz}({\rm AlN}) = -1.808 \cdot \varepsilon - 7.888 \cdot \varepsilon^2 \ \text{ for } \ \varepsilon > 0. \quad (8)$$

The basal strain for the alloy matched to a GaN layer is defined as

$$\varepsilon = (a_{\rm sub} - a)/a, \quad (9)$$

where $a_{\rm sub}$ and $a$ indicate the lattice constants of GaN and alloy layers, respectively. Note that the interface charges are shielded mainly by the defects of the device and the injected charge carriers. The number of interface charges of the experimental measurement generally varies from 20% to 80% as compared with that of the theoretical calculation.[27–29] In this paper, in order to correspond to the experimental measurement, the interface charge density is assumed to be 40% of the calculated value. The charge density shielded by the injected charge carriers is determined self-consistently at different levels of current injection. To simplify the simulation, the operating temperature and the internal absorption within the LED device are set to be 300 K and at 2000 m$^{-1}$, respectively. In this simulation, Auger recombination, Shockley–Read–Hall recombination lifetime, and radiative recombination coefficient are assumed to be $3.0 \times 10^{-31}$ cm$^6$/s, 100 ns, and $2.0 \times 10^{-11}$ cm$^3$/s, respectively. The electron mobility, hole mobility, and activating energy of Mg are defaulted to be 85 cm$^2$/V·s, 4 cm$^2$/V·s, and 180 meV. Most of the parameters used in this paper are similar to those employed in Ref. [23]. Other material parameters of the devices used in the simulation can be found in Ref. [30]. The schematic diagrams of the three structures are depicted in Fig. 1.

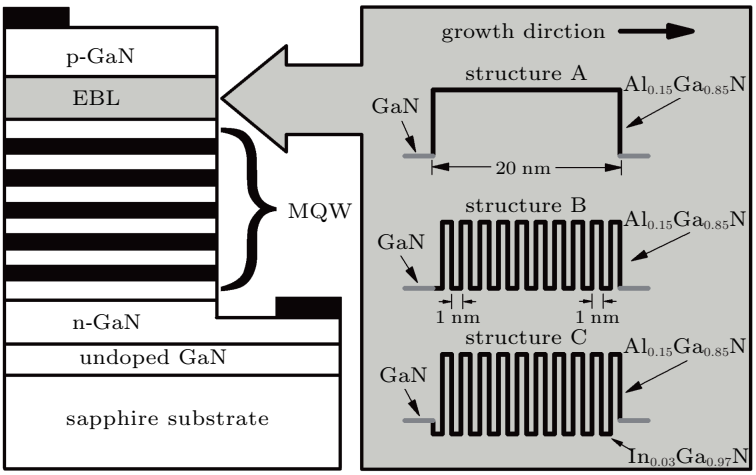



**Fig. 1.** Schematic diagram of a conventional LED with a rectangular AlGaN EBL (structure A), LED with a normal AlGaN/GaN SL EBL (structure B), and an LED with an AlGaN/InGaN SL EBL (structure C).

## 3. Simulation results and discussion

Figure 2 shows the light output powers and internal quantum efficiencies (IQEs) each as a function of current for the three LED structures. The light output powers of structure B and structure C at 200 mA are improved by 25% and 37%, respectively, as compared with that of structure A, which could be attributed to the improved efficiency droop as depicted in Fig. 2(b). In Fig. 2(b), structure A with a conventional AlGaN EBL has the lowest internal quantum efficiency and the worst efficiency droop, defined as $(\eta_{\text{peak}} - \eta_{200\text{ mA}})/\eta_{\text{peak}}$, of 31.8% which is mainly caused by severe electron leakage and poor hole injection efficiency. Note that relatively small efficiency droop (21.1%) is observed when the LED is with AlGaN/InGaN SL EBL, which is more moderate than that of the LED (25.7%) with a normal AlGaN/GaN SL EBL.

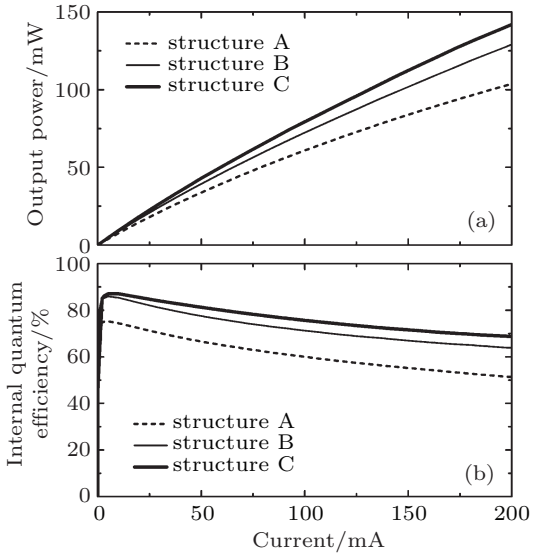



**Fig. 2.** (a) Light output powers and (b) IQEs each as a function of current for the LEDs with AlGaN EBL (structure A), AlGaN/GaN SL EBL (structure B), and AlGaN/InGaN SL EBL (structure C).

Figures 3(a), 3(c), and 3(e) show that the strengths of the electrostatic fields in the QW with different EBLs are not the same. It is obvious that the electrostatic field in the QW of structure A is strong compared with those of the other two structures especially for the last QW which is close to the EBL, while the electrostatic field in the active region of structure C is lowest in those fields. The strong electrostatic field in the QW will result in the band bending (Fig. 4), serious spatial separation of the electron and hole wavefunctions in Fig. 3(b), and hence the decrease of the radiative efficiency which will influence the internal quantum efficiency directly. Thus, structure C has an advantage over the other two structures in terms of internal quantum efficiency due to the smaller electrostatic fields in the active region. As for the LEDs with AlGaN/GaN EBL and AlGaN/InGaN EBL shown in Figs. 3(d) and 3(f), it can be found that the smaller electrostatic fields enhance the electronhole spatial overlap.

The energy-band diagrams of the three structures at 200 mA are shown in Fig. 4. In structure A, the energy band is pulled down seriously by the strong piezoelectric field induced by the charges at the interface between the last GaN barrier and AlGaN EBL. As shown in Fig. 4(a), its effective potential height for electrons in the conduction band of the AlGaN EBL (279 meV) is much smaller than those in the other two structures, and the effective potential height for holes in the valence band in the same part (297 meV) is much greater than those of the other two structures. The band bending in structure B is smaller because the superlattice structure can reduce part of the strain forces. While, as can be seen in Fig. 4(b), the electrostatic fields between the last barrier and the superlattice structure are still too large to generate an effective potential barrier height (276 meV) for holes and the accumulation of electrons in the last well is nearly unchanged. For the last GaN barrier, the compressive strain caused by $Al_{0.15}Ga_{0.85}N/In_{0.03}Ga_{0.97}N$ SL EBL is smaller than those of the other two structures. Therefore, the energy band of the last GaN barrier keeps nearly straight. As can be verified in Fig. 5(c), structure C has the lowest electron leakage and biggest hole concentrations in the QWs due to the greatest effective potential barrier height for electrons of 453 meV and the smallest effective potential barrier height for holes of 257 meV.

Figure 5 shows carrier concentrations and electron current densities of the three structures at 200 mA. As can be seen in Fig. 5(a), most electrons are confined in the last QW caused by the high polarization charge densities at the QWs/EBL interfaces, which leads to serious electron current overflow. In the meantime, the leakage current in the p-type region can recombine with holes, and thus reducing the hole injection efficiency as well as the internal quantum efficiency. On the other hand, for nitride-based materials, holes usually have values of low mobility and high effective mass and, hence, they are often difficult to inject into the active region and transport in the QW region. Thus, the hole concentration is lower than electron concentration and decreases gradually from the QW near p-side to that near n-side for structure A. In Fig. 5(b) marked improvement of hole concentration is observed compared with structure A; but the accumulation of electron in the last quantum well remains unchanged because part of the strain forces of structure B with AlGaN/GaN SL EBL are still existent. However, as indicated in Fig. 5(c), the hole concentration is improved, especially for the last QW, and the distributions of electrons and holes in the QWs become much more uniform, which is attributed to the lowest band bending caused by the strong electrostatic field at the QWs/EBL interfaces of these three structures.

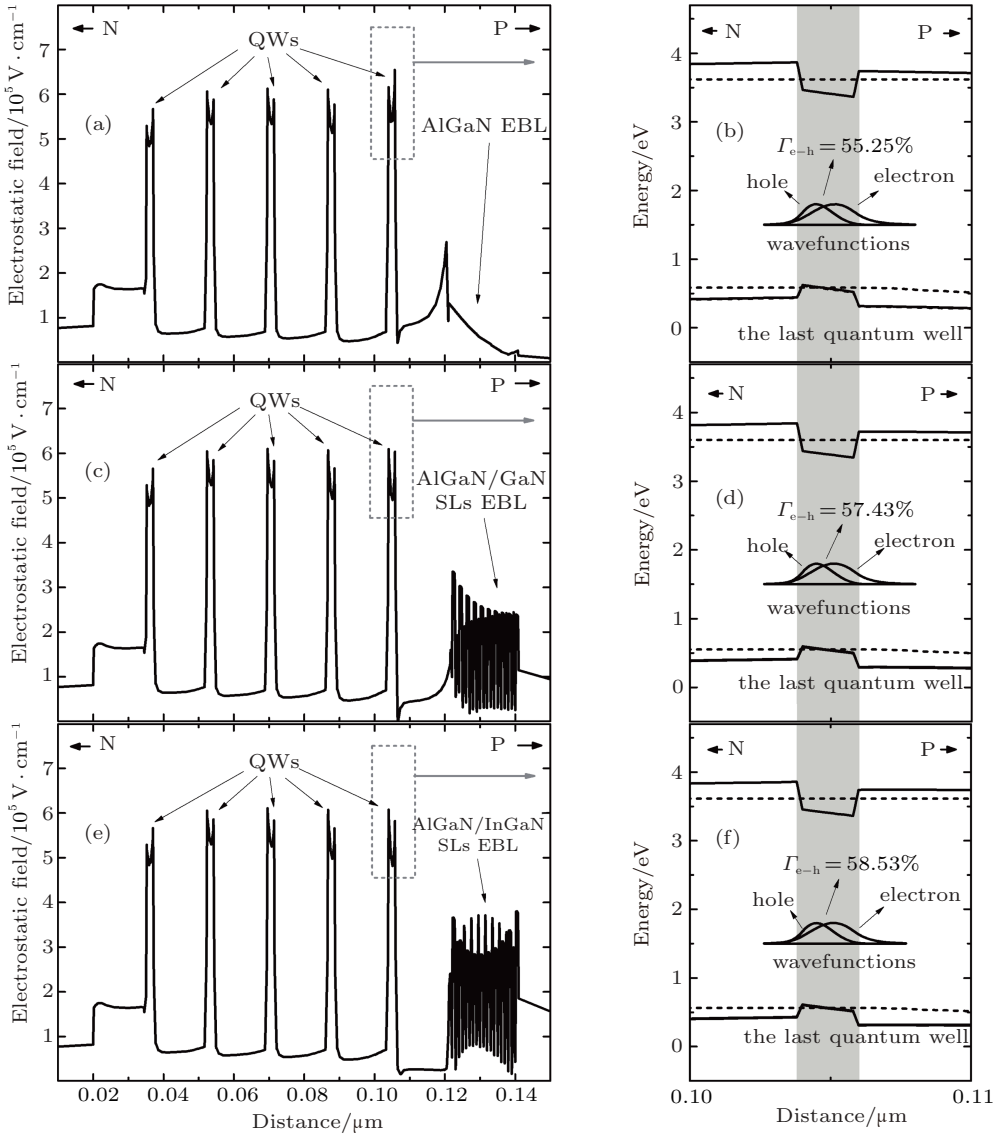



**Fig. 3.** Electrostatic fields and band wavefunctions of the LEDs with (a) and (b) AlGaN EBL (structure A), (c) and (d) AlGaN/GaN SL EBL(structure B), (e) and (f) AlGaN/InGaN SL EBL (structure C) at 200 mA.

As shown in Fig. 5(d), the electrons are injected from the n-type layers into the active region and recombine with holes in the QWs, which results in the decrease of electron current density. The electron current which escapes from the active region and then overflows into the p-layer is viewed as leakage current. Though the electron leakage currents are observed in all cases, note that structure C has the lowest electron leakage in the three structures.

Figure 6 shows the radiative recombination rates of the LEDs of the three structures at 200 mA. The horizontal positions of the LED with AlGaN EBL and AlGaN/InGaN SL EBL have been shifted slightly for better observation. For these three structures, the radiative recombination rates are mainly dominated by the QW close to the p-side layer resulting from nonuniform distributions of electrons and holes. On the other hand, for the InGaN LEDs, the optical performance is mainly dominated by the hole concentration rather than the electron concentration.[31] Therefore, in structure C, the radiative recombination rate is higher than that in the other two structures due to the enhancement of hole injection efficiency and the improvement of the efficiency of hole carrier transport. In addition, it can be found that efficiency droop at high current can be improved due to the enhancement of carrier concentrations in the QWs.

## 4. Conclusion

When the AlGaN/InGaN SL EBL is used, the hole-injection efficiency into the active region from the p-type layer can be greatly enhanced, the electron leakage can be significantly diminished, and the electrostatic fields in the active region can be considerably relieved. The LED with the newly designed structure has acquired significantly improved optical performance characteristics such as output power, and the radiative recombination rate. Furthermore, the efficiency droop of the new structure is markedly improved.

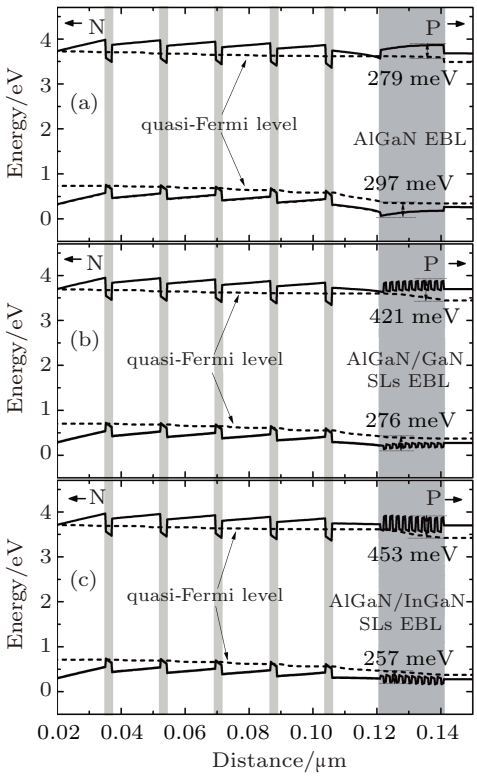



**Fig. 4.** Energy band diagrams of the LEDs with (a) AlGaN EBL, (b) AlGaN/GaN SL EBL, and (c) AlGaN/InGaN SL EBL at 200 mA.

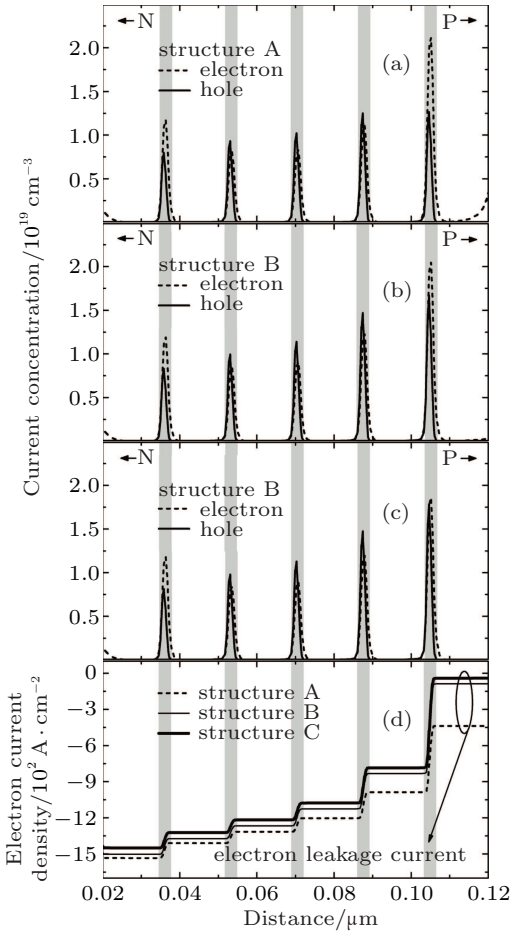



**Fig. 5.** Carrier concentrations of the LEDs with (a) AlGaN EBL, (b) AlGaN/GaN SL EBL, (c) AlGaN/InGaN SL EBL, and electron current densities (d) at 200 mA.

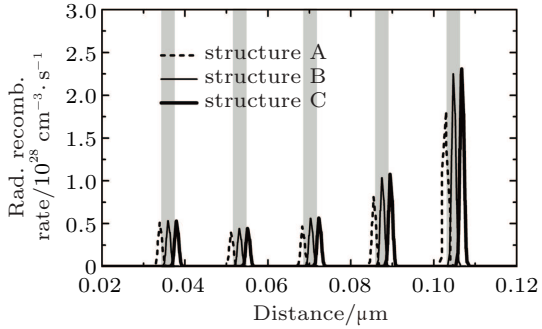



**Fig. 6.** Radiative recombination rates of the LEDs with AlGaN EBL, AlGaN/GaN SL EBL, and AlGaN/InGaN SL EBL at 20 mA.

## References


[1] Fujii T, Gao Y, Sharma R, Hu E L, DenBaars S P and Nakamura S 2004 *Appl. Phys. Lett.* **84** 855
[2] Koike M, Shibata N, Kato H and Takahashi Y 2002 *IEEE J. Sel. Topics Quantum Electron.* **8** 271
[3] Onuma T, Amaike H, Kubota M, Okamoto K, Ohta H, Ichihara J, Takasu H and Chichibu S F 2007 *Appl. Phys. Lett.* **91** 181903
[4] Shen Y C, Mueller G O, Watanabe S, Gardner N F, Munkholm A and Krames M R 2007 *Appl. Phys. Lett.* **91** 141101
[5] Su Y K, Chang S J, Wei S C, Chuang R W, Chen S M and Li W L 2005 *IEEE Electron Dev. Lett.* **26** 891
[6] Gong Z, Jin S, Chen Y, McKendry J, Massoubre D, Watson I M, Gu E and Dawson M D 2010 *J. Appl. Phys.* **107** 013103
[7] Kim M H, Schubert M F, Dai Q, Kim J K, Schubert E F, Piprek J and Park Y 2007 *Appl. Phys. Lett.* **91** 183507
[8] Zhao H, Liu G, Arif R A and Tansu N 2010 *Solid-State Electron.* **54** 1119
[9] Vampola K J, Iza M, Keller S, DenBaars S P and Nakamura S 2009 *Appl. Phys. Lett.* **94** 061116
[10] Ni X, Fan Q, Shimada R, Özgür Ü and Morkoç H 2008 *Appl. Phys. Lett.* **93** 171113
[11] Yen S H, Tsai M L, Tsai M C, Chang S J and Kuo Y K 2010 *IEEE Photon. Technol. Lett.* **22** 1787
[12] Lu T P, Li S T, Zhang K, Liu C, Xiao G W, Zhou Y G, Zheng S W, Yin Y A, Wu L J, Wang H L and Yang X D 2011 *Chin. Phys. B* **20** 098503
[13] Kuo Y K, Shih Y H, Tsai M C and Chang J Y 2011 *IEEE Photon. Technol. Lett.* **23** 1630
[14] Wang T H and Xu J L 2012 *Chin. Phys. B* **21** 128504
[15] Rozhansky I V and Zakheim D A 2006 *Phys. Stat. Sol.* **3** 2160
[16] Xie J, Ni X, Fan Q, Shimada R, Özgür Ü and Morkoç H 2008 *Appl. Phys. Lett.* **93** 121107
[17] Rozhansky I V and Zakheim D A 2006 *Semiconductors* **40** 839
[18] Liu C, Ren Z W, Chen X, Zhao B J, Wang X F, Yin Y A and Li S T 2013 *Chin. Phys. B* **22** 058502
[19] Wu L J, Li S T, Liu C, Wang H L, Lu T P, Zhang K, Xiao G W, Zhou Y G, Zheng S W, Yin Y A and Yang X D 2012 *Chin. Phys. B* **21** 068506
[20] Kumakura K and Kobayashi N 1999 *Jpn. J. Appl. Phys.* **38** L1012
[21] Gong C C, Fan G H, Zhang Y Y, Xu Y Q, Liu X P, Zheng S W, Yao G R and Zhou D T 2012 *Chin. Phys. B* **21** 068505
[22] Li J C, Yang W H, Li S P, Chen H Y, Liu D Y and Kang J Y 2009 *Appl. Phys. Lett.* **95** 151113
[23] Zhang Y Y and Yin Y A 2011 *Appl. Phys. Lett.* **99** 221103
[24] Kuo Y K, Wang T H and Chang J Y 2012 *Appl. Phys. Lett.* **100** 031112
[25] APSYS by Crosslight Software Inc., Burnaby, Canada, available at http://www.crosslight.com
[26] Fiorentini V, Bernardini F and Ambacher O 2002 *Appl. Phys. Lett.* **80** 1204
[27] Chichibu S F, Abare A C, Minsky M S, Keller S, Fleischer S B, Bowers J E, Hu E, Mishra U K, Coldren L A, DenBaars S P and Sota T 1998 *Appl. Phys. Lett.* **73** 2006
[28] Renner F, Kiesel P, Döhler G H, Kneissl M, Van de Walle C G and Johnson N M 2002 *Appl. Phys. Lett.* **81** 490
[29] Zhang H, Miller E J, Yu E T, Poblenz C and Speck J S 2004 *Appl. Phys. Lett.* **84** 4644
[30] Kuo Y K, Tsai M C, Yen S H, Hsu T C and Shen Y J 2010 *IEEE J. Quantum Electron.* **46** 1214
[31] Kuo Y K, Chang J Y, Tsai M C and Yen S H 2009 *Appl. Phys. Lett.* **95** 011116